High-scale validity of 2HDM scenarios: Study using LHC data.

Nabarun Chakrabarty
HRI, Allahabad

September 10, 2015, IPMU

JHEP12(2014)166: NC, Ujjal Kmar Dey, Biswarup Mukhopadhyaya
and
Phys. Rev. D 92, 015002 (2015): NC, Dilip Kumar Ghosh, Biswarup Mukhopadhyaya, Ipsita Saha

Outline

- High-scale validity of a Type-II 2HDM scenario and the role of LHC data.

Outline

- High-scale validity of a Type-II 2HDM scenario and the role of LHC data.
- Dark matter and a radiative neutrino mass in a 2HDM.

Vacuum stability: Motivating the 2HDM

- In the Standard Model (SM), the stability of the electroweak vacuum is sensitive to the values of the masses of the Higgs and the top-quark. In particular, higher M_t render the vacuum unstable well below the Planck scale (M_{Pl}).

Vacuum stability: Motivating the 2HDM

- In the Standard Model (SM), the stability of the electroweak vacuum is sensitive to the values of the masses of the Higgs and the top-quark. In particular, higher M_t render the vacuum unstable well below the Planck scale (M_{Pl}).

- Could it help to have an extra scalar doublet?

Vacuum stability: Motivating the 2HDM

- In the Standard Model (SM), the stability of the electroweak vacuum is sensitive to the values of the masses of the Higgs and the top-quark. In particular, higher M_t render the vacuum unstable well below the Planck scale (M_{Pl}).

- Could it help to have an extra scalar doublet?

- Pros: Rich phenomenology, Dark Matter (DM) canditate in special cases.

Vacuum stability: Motivating the 2HDM

- In the Standard Model (SM), the stability of the electroweak vacuum is sensitive to the values of the masses of the Higgs and the top-quark. In particular, higher M_t render the vacuum unstable well below the Planck scale (M_{Pl}).
- Could it help to have an extra scalar doublet?
- Pros: Rich phenomenology, Dark Matter (DM) canditate in special cases.
- Cons: Additional doublets $\longrightarrow$ Additional quartic couplings $\longrightarrow$ Fast rise of such couplings $\longrightarrow$ threat to perturbativity.

Vacuum stability: Motivating the 2HDM

- In the Standard Model (SM), the stability of the electroweak vacuum is sensitive to the values of the masses of the Higgs and the top-quark. In particular, higher M_t render the vacuum unstable well below the Planck scale (M_{Pl}).
- Could it help to have an extra scalar doublet?
- Pros: Rich phenomenology, Dark Matter (DM) canditate in special cases.
- Cons: Additional doublets $\longrightarrow$ Additional quartic couplings $\longrightarrow$ Fast rise of such couplings $\longrightarrow$ threat to perturbativity.
- Our goal: To see if there is a balance between these extremes, modulo constraints from LHC and DM experiments.

Model: Type II 2HDM

- Most general renormalizable scalar potential for two doublets Φ_1 and Φ_2, each having hypercharge $(+1)$

$$
\begin{aligned}
V(\Phi_1,\Phi_2) = {} & m_{11}^2\,\Phi_1^\dagger\Phi_1 + m_{22}^2\,\Phi_2^\dagger\Phi_2 - m_{12}^2\,\left(\Phi_1^\dagger\Phi_2 + \Phi_2^\dagger\Phi_1\right) \\
& + \frac{\lambda_1}{2}\left(\Phi_1^\dagger\Phi_1\right)^2 + \frac{\lambda_2}{2}\left(\Phi_2^\dagger\Phi_2\right)^2 \\
& + \lambda_3\,\Phi_1^\dagger\Phi_1\,\Phi_2^\dagger\Phi_2 + \lambda_4\,\Phi_1^\dagger\Phi_2\,\Phi_2^\dagger\Phi_1 + \frac{\lambda_5}{2}\left[\left(\Phi_1^\dagger\Phi_2\right)^2 + \left(\Phi_2^\dagger\Phi_1\right)^2\right] \\
& + \lambda_6\,\Phi_1^\dagger\Phi_1\,\left(\Phi_1^\dagger\Phi_2 + \Phi_2^\dagger\Phi_1\right) + \lambda_7\,\Phi_2^\dagger\Phi_2\,\left(\Phi_1^\dagger\Phi_2 + \Phi_2^\dagger\Phi_1\right)
\end{aligned}
$$

Model: Type II 2HDM

- Most general renormalizable scalar potential for two doublets Φ_1 and Φ_2, each having hypercharge $(+1)$

$$
\begin{aligned}
V(\Phi_1,\Phi_2) &= m_{11}^2\,\Phi_1^\dagger\Phi_1 + m_{22}^2\,\Phi_2^\dagger\Phi_2 - m_{12}^2\,\left(\Phi_1^\dagger\Phi_2 + \Phi_2^\dagger\Phi_1\right) \\
&+ \frac{\lambda_1}{2}\left(\Phi_1^\dagger\Phi_1\right)^2 + \frac{\lambda_2}{2}\left(\Phi_2^\dagger\Phi_2\right)^2 \\
&+ \lambda_3\,\Phi_1^\dagger\Phi_1\,\Phi_2^\dagger\Phi_2 + \lambda_4\,\Phi_1^\dagger\Phi_2\,\Phi_2^\dagger\Phi_1 + \frac{\lambda_5}{2}\left[\left(\Phi_1^\dagger\Phi_2\right)^2 + \left(\Phi_2^\dagger\Phi_1\right)^2\right] \\
&+ \lambda_6\,\Phi_1^\dagger\Phi_1\,\left(\Phi_1^\dagger\Phi_2 + \Phi_2^\dagger\Phi_1\right) + \lambda_7\,\Phi_2^\dagger\Phi_2\,\left(\Phi_1^\dagger\Phi_2 + \Phi_2^\dagger\Phi_1\right)
\end{aligned}
$$

- The doublets acquire vevs through spontaneous symmetry breaking.

$$
\langle\Phi_1\rangle = \frac{1}{\sqrt{2}}\begin{pmatrix} 0 \\ v_1 \end{pmatrix}, \quad \langle\Phi_2\rangle = \frac{1}{\sqrt{2}}\begin{pmatrix} 0 \\ v_2 \end{pmatrix}, \tag{1}
$$

Model: Type II 2HDM

- Most general renormalizable scalar potential for two doublets Φ_1 and Φ_2, each having hypercharge $(+1)$

$$\begin{aligned} V(\Phi_1,\Phi_2) &= m_{11}^2\,\Phi_1^\dagger\Phi_1 + m_{22}^2\,\Phi_2^\dagger\Phi_2 - m_{12}^2\,\left(\Phi_1^\dagger\Phi_2+\Phi_2^\dagger\Phi_1\right) \\ &+ \frac{\lambda_1}{2}\left(\Phi_1^\dagger\Phi_1\right)^2 + \frac{\lambda_2}{2}\left(\Phi_2^\dagger\Phi_2\right)^2 \\ &+ \lambda_3\,\Phi_1^\dagger\Phi_1\,\Phi_2^\dagger\Phi_2 + \lambda_4\,\Phi_1^\dagger\Phi_2\,\Phi_2^\dagger\Phi_1 + \frac{\lambda_5}{2}\left[\left(\Phi_1^\dagger\Phi_2\right)^2+\left(\Phi_2^\dagger\Phi_1\right)^2\right] \\ &+ \lambda_6\,\Phi_1^\dagger\Phi_1\,\left(\Phi_1^\dagger\Phi_2+\Phi_2^\dagger\Phi_1\right) + \lambda_7\,\Phi_2^\dagger\Phi_2\,\left(\Phi_1^\dagger\Phi_2+\Phi_2^\dagger\Phi_1\right) \end{aligned}$$

- The doublets acquire vevs through spontaneous symmetry breaking.

$$\langle\Phi_1\rangle = \frac{1}{\sqrt{2}}\begin{pmatrix} 0 \\ v_1 \end{pmatrix}, \quad \langle\Phi_2\rangle = \frac{1}{\sqrt{2}}\begin{pmatrix} 0 \\ v_2 \end{pmatrix}, \tag{1}$$

- Enlarged scalar spectrum: Mutually conjugate pair of charged scalars ($H^\pm$), two neutral scalars (H, h) and a neutral pseudoscalar (A).

Model: Type II 2HDM

- Fermions must couple to any one of the doublets in order to suppress FCNCs at the tree level. This can be achieved by invoking a $\mathbb{Z}_2$ symmetry.

Model: Type II 2HDM

- Fermions must couple to any one of the doublets in order to suppress FCNCs at the tree level. This can be achieved by invoking a $\mathbb{Z}_2$ symmetry.
- For the $\mathbb{Z}_2$ charge assignment $\Phi_1 \rightarrow -\Phi_1$ and $\psi_R^i \rightarrow -\psi_R^i$ (where ψ is a charged lepton or a down type quark), down-type quarks and leptons couple to Φ_1. Up-type quarks couple to Φ_2. (Type-II 2HDM).

Model: Type II 2HDM

- Fermions must couple to any one of the doublets in order to suppress FCNCs at the tree level. This can be achieved by invoking a $\mathbb{Z}_2$ symmetry.
- For the $\mathbb{Z}_2$ charge assignment $\Phi_1 \to -\Phi_1$ and $\psi_R^i \to -\psi_R^i$ (where ψ is a charged lepton or a down type quark), down-type quarks and leptons couple to Φ_1. Up-type quarks couple to Φ_2. (Type-II 2HDM).
- The Analytic forms of the 2HDM beta functions depend on the 2HDM "Type".

Model: Type II 2HDM

- Fermions must couple to any one of the doublets in order to suppress FCNCs at the tree level. This can be achieved by invoking a $\mathbb{Z}_2$ symmetry.
- For the $\mathbb{Z}_2$ charge assignment $\Phi_1 \to -\Phi_1$ and $\psi^i_R \to -\psi^i_R$ (where ψ is a charged lepton or a down type quark), down-type quarks and leptons couple to Φ_1. Up-type quarks couple to Φ_2. (Type-II 2HDM).
- The Analytic forms of the 2HDM beta functions depend on the 2HDM "Type".
- We illustrate our findings in context of a Type II 2HDM.

Constraints and analysis strategy

- We demand $m_h \sim 125$ GeV to conform with the Higgs discovery@LHC and $m_{H^+} \geq 315$ GeV to avoid flavor constraints.

Constraints and analysis strategy

- We demand $m_h \sim 125$ GeV to conform with the Higgs discovery@LHC and $m_{H^+} \geq 315$ GeV to avoid flavor constraints.

- The theoretical constraints stemming from perturbativity, unitarity and vacuum stability imposed at the electroweak (EW) scale, $\mu = M_t$.

Constraints and analysis strategy

- We demand $m_h \sim 125$ GeV to conform with the Higgs discovery@LHC and $m_{H^+} \geq 315$ GeV to avoid flavor constraints.
- The theoretical constraints stemming from perturbativity, unitarity and vacuum stability imposed at the electroweak (EW) scale, $\mu = M_t$.
- Parameter points clearing these constraints then allowed to evolve under Renormalisation Group (RG). Theoretical constraints imposed at each scale up to some desired cut-off $\rightarrow$ EW scale gets parameter space constrained.

Constraints and analysis strategy

- We demand $m_h \sim 125$ GeV to conform with the Higgs discovery@LHC and $m_{H^+} \geq 315$ GeV to avoid flavor constraints.
- The theoretical constraints stemming from perturbativity, unitarity and vacuum stability imposed at the electroweak (EW) scale, $\mu = M_t$.
- Parameter points clearing these constraints then allowed to evolve under Renormalisation Group (RG). Theoretical constraints imposed at each scale up to some desired cut-off $\rightarrow$ EW scale gets parameter space constrained.
- Higgs signal strength constraints at 2σ further imposed.

Results: Exact $\mathbb{Z}_2$ symmetry

- $m_{12}, \lambda_6, \lambda_7 = 0$, $\rightarrow$ A 123-127 GeV h difficult to obtain for higher $\tan\beta$.

Results: Exact $\mathbb{Z}_2$ symmetry

- $m_{12}, \lambda_6, \lambda_7 = 0$, $\rightarrow$ A 123-127 GeV h difficult to obtain for higher $\tan\beta$.
- λ_i become non-perturbative around 10 TeV. Parameter space of λ_i gets tight at the EW scale $\rightarrow$ Tight bounds on the scalar masses.

Results: Exact $\mathbb{Z}_2$ symmetry

- $m_{12}, \lambda_6, \lambda_7 = 0, \rightarrow$ A 123-127 GeV h difficult to obtain for higher $\tan\beta$.
- λ_i become non-perturbative around 10 TeV. Parameter space of λ_i gets tight at the EW scale $\rightarrow$ Tight bounds on the scalar masses.

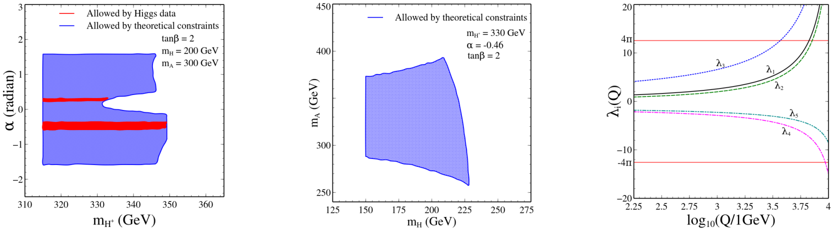

Figure: Theoretically allowed parameter spaces at $\Lambda_{UV} = 1$ TeV, $\tan\beta = 2$ and $m_{12} = 0$ GeV for $M_t = 173.1$ GeV. Running of λ_i also shown.

Results: Exact $\mathbb{Z}_2$ symmetry

- $m_{12}, \lambda_6, \lambda_7 = 0$, $\rightarrow$ A 123-127 GeV h difficult to obtain for higher $\tan\beta$.

- λ_i become non-perturbative around 10 TeV. Parameter space of λ_i gets tight at the EW scale $\rightarrow$ Tight bounds on the scalar masses.

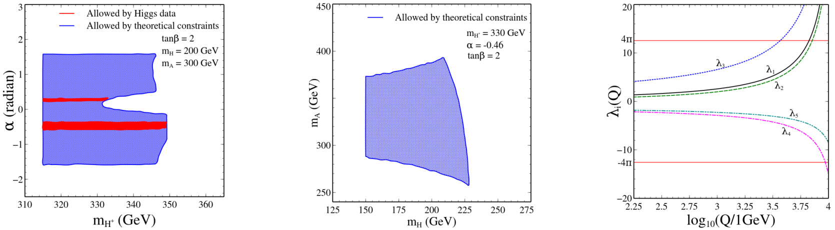

Figure: Theoretically allowed parameter spaces at $\Lambda_{UV} = 1$ TeV, $\tan\beta = 2$ and $m_{12} = 0$ GeV for $M_t = 173.1$ GeV. Running of λ_i also shown.

- Motivates one to look beyond exact $\mathbb{Z}_2$ symmetry.

Results: Softly broken $\mathbb{Z}_2$ symmetry

- Include $m_{12} \neq 0$ in the scalar potential while keeping $\lambda_6, \lambda_7 = 0$.
  $\tan\beta = 2, 10, 20$ and $m_{12} = 200, 1000$ GeV are the benchmarks chosen.

Results: Softly broken $\mathbb{Z}_2$ symmetry

- Include $m_{12} \neq 0$ in the scalar potential while keeping $\lambda_6, \lambda_7 = 0$.
  $\tan\beta = 2, 10, 20$ and $m_{12} = 200, 1000$ GeV are the benchmarks chosen.

- The theoretical constraints found intact upto M_{Pl}, though for a restricted region in the parameter space. For one such benchmark,

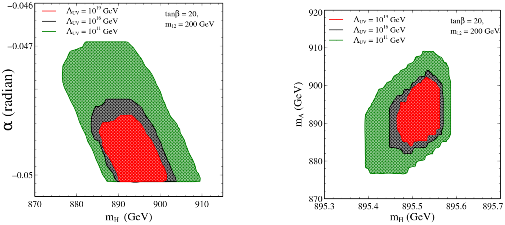

Figure: The allowed parameter spaces in the soft $\mathbb{Z}_2$ breaking case for $\Lambda_{UV} = 10^{11}$ (green), 10^{16} (grey) and 10^{19} GeV (red).

Results: Softly broken $\mathbb{Z}_2$ symmetry

- Include $m_{12} \neq 0$ in the scalar potential while keeping $\lambda_6, \lambda_7 = 0$. $\tan\beta = 2, 10, 20$ and $m_{12} = 200, 1000$ GeV are the benchmarks chosen.

- The theoretical constraints found intact upto M_{Pl}, though for a restricted region in the parameter space. For one such benchmark,

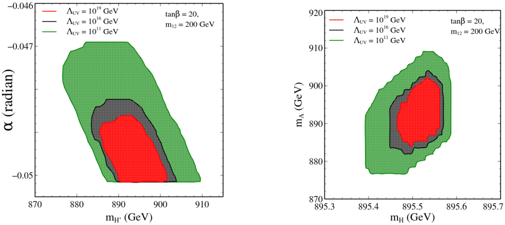

Figure: The allowed parameter spaces in the soft $\mathbb{Z}_2$ breaking case for $\Lambda_{UV} = 10^{11}$ (green), 10^{16} (grey) and 10^{19} GeV (red).

- Fixing m_{12} induces a high degree of correlation amongst the non-standard scalar masses. They loom around the TeV scale for the benchmarks taken.

Results: *Softly* broken $\mathbb{Z}_2$ symmetry

- Unlike the SM, the electroweak vacuum is rendered stable even for high values of M_t.

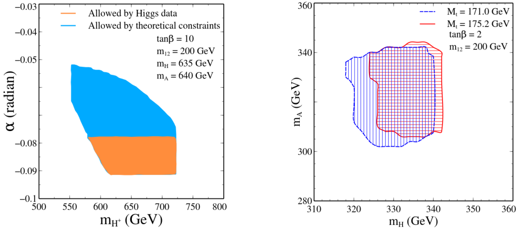

Figure: The first two figures describe regions in the $m_{H^\pm}$-α plane allowed by the Higgs data in the soft $\mathbb{Z}_2$ breaking case. The last one depicts parameter spaces in m_H-m_A plane for two different values of M_t.

Results: *Softly* broken $\mathbb{Z}_2$ symmetry

- Unlike the SM, the electroweak vacuum is rendered stable even for high values of M_t.

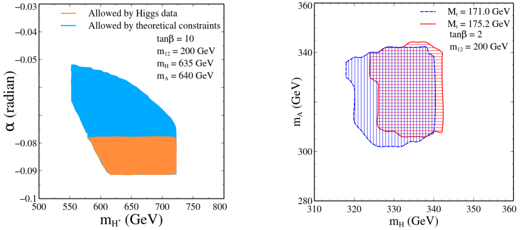

Figure: The first two figures describe regions in the $m_{H^{\pm}}$-α plane allowed by the Higgs data in the soft $\mathbb{Z}_2$ breaking case. The last one depicts parameter spaces in m_H-m_A plane for two different values of M_t.

- Higgs data from the LHC imposes $\alpha \sim \beta$ - $\frac{\pi}{2}$, i.e. takes the 2HDM near the *alignment limit*.

Results: $\mathbb{Z}_2$ symmetry broken by *hard* terms

- $\lambda_6, \lambda_7 \neq 0$. $\lambda_1(M_t) = 0.02$ and $\lambda_6(M_t) = \lambda_7(M_t)$ for computational convenience.

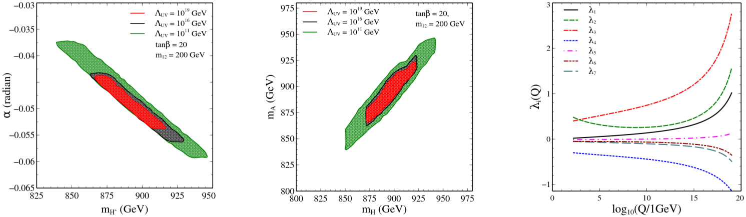

Figure: The allowed parameter spaces for $\Lambda_{UV} = 10^{11}$ (green), 10^{16} (grey) and 10^{19} GeV (red), in the $\lambda_6, \lambda_7 \neq 0$ case. The $\tan\beta$ and m_{12} values are shown in the plots.

Results: $\mathbb{Z}_2$ symmetry broken by *hard* terms

- $\lambda_6, \lambda_7 \neq 0$. $\lambda_1(M_t) = 0.02$ and $\lambda_6(M_t) = \lambda_7(M_t)$ for computational convenience.

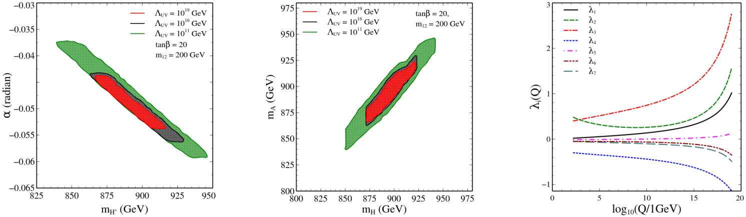

Figure: The allowed parameter spaces for $\Lambda_{UV} = 10^{11}$ (green), 10^{16} (grey) and 10^{19} GeV (red), in the $\lambda_6, \lambda_7 \neq 0$ case. The $\tan\beta$ and m_{12} values are shown in the plots.

- Larger parameter space opens up ensuring validity up to high scales. Thus, a Type-II 2HDM could be valid upto M_{Pl} only if the $\mathbb{Z}_2$ symmetry is broken either by *soft* or *hard* terms.

The Model: Inert doublet + Heavy neutrinos

- An additional Higgs doublet (Φ_2) and three heavy neutrinos (N_i), in addition to the SM fields, .

The Model: Inert doublet + Heavy neutrinos

- An additional Higgs doublet (Φ_2) and three heavy neutrinos (N_i), in addition to the SM fields, .
- An unbroken Z_2 symmetry, under which Φ_2 and N_i are odd while all other SM particles are even. Keeps Φ_2 free from a vacuum expectation value (vev).

The Model: Inert doublet + Heavy neutrinos

- An additional Higgs doublet (Φ_2) and three heavy neutrinos (N_i), in addition to the SM fields, .
- An unbroken Z_2 symmetry, under which Φ_2 and N_i are odd while all other SM particles are even. Keeps Φ_2 free from a vacuum expectation value (vev).
- The RH neutrinos play the role of generating a neutrino mass radiatively.

The Model: Inert doublet + Heavy neutrinos

- The relevant Yukawa and mass terms are

$$-\mathcal{L}_Y = (y_{ij}\bar{N}_i\tilde{\Phi}_2^\dagger\ell_j + h.c) + \frac{M_i}{2}\left(\bar{N}_i^c N_i + h.c\right), (i,j=1,2,3) \qquad (2)$$

The Model: Inert doublet + Heavy neutrinos

- The relevant Yukawa and mass terms are

$$-\mathcal{L}_Y \quad = \quad (y_{ij}\bar{N}_i\tilde{\Phi}_2^\dagger \ell_j + h.c) + \frac{M_i}{2}\left(\bar{N}_i^c N_i + h.c\right), (i,j = 1,2,3) \qquad (2)$$

- In the inert limit,

$$\Phi_1 = \begin{pmatrix} G^+ \\ \frac{1}{\sqrt{2}}(v + h + iG) \end{pmatrix} \text{ and, } \Phi_2 = \begin{pmatrix} H^+ \\ \frac{1}{\sqrt{2}}(H + iA) \end{pmatrix} \qquad (3)$$

We illustrate our results with H as the DM canditate.

- Correct relic density is achieved in two mass regions.

The Model: Inert doublet + Heavy neutrinos

- The relevant Yukawa and mass terms are

$$-\mathcal{L}_Y \quad = \quad \left(y_{ij}\bar{N}_i\tilde{\Phi}_2^\dagger\ell_j + h.c\right) + \frac{M_i}{2}\left(\bar{N}_i^c N_i + h.c\right), (i,j = 1,2,3) \qquad (2)$$

- In the inert limit,

$$\Phi_1 = \begin{pmatrix} G^+ \\ \frac{1}{\sqrt{2}}(v + h + iG) \end{pmatrix} \text{ and, } \Phi_2 = \begin{pmatrix} H^+ \\ \frac{1}{\sqrt{2}}(H + iA) \end{pmatrix} \qquad (3)$$

We illustrate our results with H as the DM canditate.

- Correct relic density is achieved in two mass regions.

- $50\ \mathrm{GeV} < \mathrm{M_H} < 90\ \mathrm{GeV}$: s-channel DM annihilation through h exchange, and t-channel annihilation through A and $H^\pm$ exchange (Hambye 2009, Arhrib 2013).

The Model: Inert doublet + Heavy neutrinos

- The relevant Yukawa and mass terms are

$$-\mathcal{L}_Y = (y_{ij}\bar{N}_i\tilde{\Phi}_2^\dagger \ell_j + h.c) + \frac{M_i}{2}\left(\bar{N}_i^c N_i + h.c\right), (i,j = 1,2,3) \quad (2)$$

- In the inert limit,

$$\Phi_1 = \begin{pmatrix} G^+ \\ \frac{1}{\sqrt{2}}(v + h + iG) \end{pmatrix} \text{ and, } \Phi_2 = \begin{pmatrix} H^+ \\ \frac{1}{\sqrt{2}}(H + iA) \end{pmatrix} \quad (3)$$

We illustrate our results with H as the DM canditate.

- Correct relic density is achieved in two mass regions.

- $50 \text{ GeV} < \mathrm{M_H} < 90 \text{ GeV}$: s-channel DM annihilation through h exchange, and t-channel annihilation through A and $H^\pm$ exchange (Hambye 2009, Arhrib 2013).

- $M_H > 500 \text{ GeV}$: Co-annihilations among H, A and $H^\pm$ (Arhrib 2013).

The Model: Inert doublet + Heavy neutrinos

- Loop-induced light neutrino mass matrix (Ma,2006km),

The Model: Inert doublet + Heavy neutrinos

- Loop-induced light neutrino mass matrix (Ma,2006km),

$$\mathcal{M}^{\nu}_{ij} = \sum_{k=1}^{3} \frac{y_{ik} y_{jk} M_k}{16\pi^2} \left[\frac{M_H^2}{M_H^2 - M_k^2} \ln \frac{M_H^2}{M_k^2} - \frac{M_A^2}{M_A^2 - M_k^2} \ln \frac{M_A^2}{M_k^2} \right] \tag{4}$$

- Benchmarks of M consistent with leptogenesis, (a) $M = 110\ \mathrm{TeV}$ and (b) $M = 10^9\ \mathrm{TeV}$ (Pilaftsis,1997; Hambye,2009). N_i-H co-annihilation ruled out.

The Model: Inert doublet + Heavy neutrinos

- Loop-induced light neutrino mass matrix (Ma,2006km),

$$\mathcal{M}^{\nu}_{ij} = \sum_{k=1}^{3} \frac{y_{ik} y_{jk} M_k}{16\pi^2} \left[\frac{M_H^2}{M_H^2 - M_k^2} \ln \frac{M_H^2}{M_k^2} - \frac{M_A^2}{M_A^2 - M_k^2} \ln \frac{M_A^2}{M_k^2} \right] \tag{4}$$

- Benchmarks of M consistent with leptogenesis, (a) $M = 110\ \mathrm{TeV}$ and (b) $M = 10^9\ \mathrm{TeV}$ (Pilaftsis,1997; Hambye,2009). N_i-H co-annihilation ruled out.

- Effect of N_i in the beta functions only considered above the threshold M.

The Model: Inert doublet + Heavy neutrinos

- Loop-induced light neutrino mass matrix (Ma,2006km),

$$\mathcal{M}^{\nu}_{ij} = \sum_{k=1}^{3} \frac{y_{ik} y_{jk} M_k}{16\pi^2} \left[\frac{M_H^2}{M_H^2 - M_k^2} \ln \frac{M_H^2}{M_k^2} - \frac{M_A^2}{M_A^2 - M_k^2} \ln \frac{M_A^2}{M_k^2} \right] \qquad (4)$$

- Benchmarks of M consistent with leptogenesis, (a) $M = 110 \ \mathrm{TeV}$ and (b) $M = 10^9 \ \mathrm{TeV}$ (Pilaftsis,1997; Hambye,2009). N_i-H co-annihilation ruled out.

- Effect of N_i in the beta functions only considered above the threshold M.
$M = 10$ TeV $\longrightarrow y_\nu = O(10^{-5}) \longrightarrow$ No effect on RG evolution.
$M = 10^9$ TeV $\longrightarrow y_\nu = O(1) \longrightarrow$ Appreciable effect on RG evolution.

$$16\pi^2 \frac{d\lambda_2}{dt}\bigg|_{IDM+RH} = 16\pi^2 \frac{d\lambda_2}{dt}\bigg|_{IDM} + 4\lambda_2 y_\nu^2 - 4y_\nu^4 \qquad (5)$$

Constraints: Theory and Experiments

- Fix $m_h = 125$ GeV, Requirement of perturbativity, unitarity and vacuum stability at each scale up to some given cut-off.

Constraints: Theory and Experiments

- Fix $m_h = 125$ GeV, Requirement of perturbativity, unitarity and vacuum stability at each scale up to some given cut-off.
- $\mathcal{M}_\nu \sim \mathcal{O}(0.1\ \mathrm{eV})$ consistent with neutrino oscillation data.

Constraints: Theory and Experiments

- Fix $m_h = 125$ GeV, Requirement of perturbativity, unitarity and vacuum stability at each scale up to some given cut-off.

- $\mathcal{M}_\nu \sim \mathcal{O}(0.1\ \mathrm{eV})$ consistent with neutrino oscillation data.

- Latest PLANCK data gives

$$\Omega_{\mathrm{DM}} h^2 = 0.1199 \pm 0.0027 \tag{6}$$

3σ deviation from the central value permitted. Bound on nucleon-DM scattering cross section given by LUX obeyed.

Constraints: Theory and Experiments

- Fix $m_h = 125$ GeV, Requirement of perturbativity, unitarity and vacuum stability at each scale up to some given cut-off.

- $\mathcal{M}_\nu \sim \mathcal{O}(0.1 \text{ eV})$ consistent with neutrino oscillation data.

- Latest PLANCK data gives

$$\Omega_{\rm DM} h^2 = 0.1199 \pm 0.0027 \tag{6}$$

  3σ deviation from the central value permitted. Bound on nucleon-DM scattering cross section given by LUX obeyed.

- Higgs signal strengths from ATLAS and CMS satisfied at 2σ.

Results

- Vary $50\ \mathrm{GeV} < \mathrm{M_H} < 90\ \mathrm{GeV}$, $80\ \mathrm{GeV} < \mathrm{M_{H^\pm}}, \mathrm{M_A}$. Fix λ_2 and M at two chosen benchmarks.
- Stability upto the Planck scale achieved, a radiative neutrino mass, relic density and direct detection cross section in the correct ballpark.

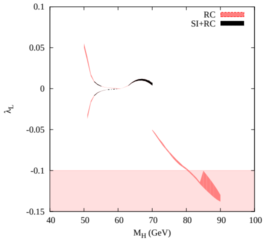

Results: $50 \text{ GeV} < M_H < 90 \text{ GeV}$

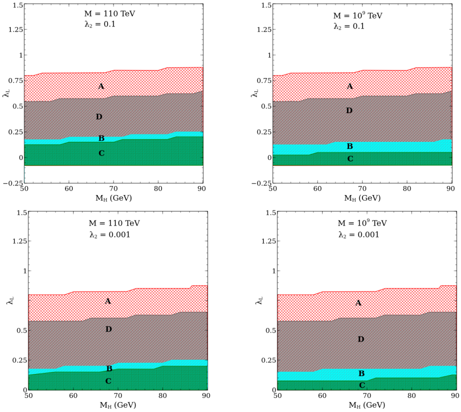

Figure: Regions compatible with the theoretical constraints for $M = 110$ TeV (left panel) and 10^9 TeV (right panel) with three different choices of Λ_{UV} and two values of λ_2. The regions denoted by A (red), B (cyan) and C (green) obey these constraints up to $\Lambda_{UV} = 10^6$, 10^{16} and 10^{19} GeV respectively. The grey region denoted by D keeps the Higgs to diphoton signal strength within 2σ limits of the current data.

Results: 50 GeV $< \mathrm{M_H} <$ 90 GeV

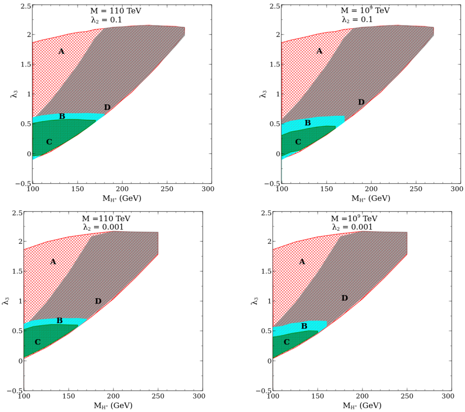

- Perturbative unitarity $\rightarrow$ *Tight upper bound on scalar masses + upper bound on λ_2*
- Vacuum stability $\rightarrow$ *Affected by λ_2*

Results: $M_H > 500$ GeV

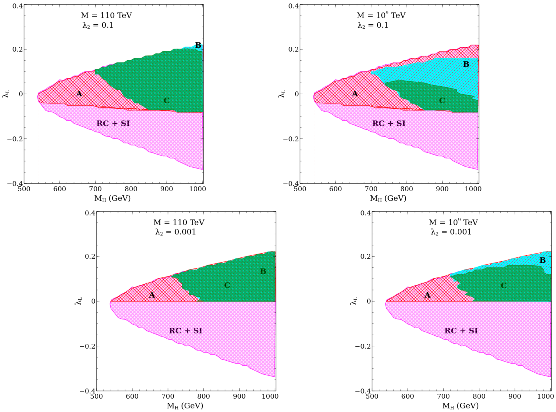

- $M = 10^9$ TeV $\longrightarrow y_\nu = O(1) \rightarrow \lambda_2(\mu)$ *starts approaching instability beyond the scale* M.

Conclusions

- In the first part, high-scale stability of the Type-II 2HDM scenario was examined.

Conclusions

- In the first part, high-scale stability of the Type-II 2HDM scenario was examined.
- The *exact* $\mathbb{Z}_2$ symmetric model non-perturbative beyond 10 TeV. However, a broken $\mathbb{Z}_2$ needed to salvage high-scale validity all the way up to the M_{Pl}.

Conclusions

- In the first part, high-scale stability of the Type-II 2HDM scenario was examined.
- The *exact* $\mathbb{Z}_2$ symmetric model non-perturbative beyond 10 TeV. However, a broken $\mathbb{Z}_2$ needed to salvage high-scale validity all the way up to the M_{Pl}.
- In the second part, we have examined the high-scale validity of a scenario that (a) offers a scalar dark matter, (b) radiatively generates mass for the light neutrinos.

Conclusions

- In the first part, high-scale stability of the Type-II 2HDM scenario was examined.
- The *exact* $\mathbb{Z}_2$ symmetric model non-perturbative beyond 10 TeV. However, a broken $\mathbb{Z}_2$ needed to salvage high-scale validity all the way up to the M_{Pl}.
- In the second part, we have examined the high-scale validity of a scenario that (a) offers a scalar dark matter, (b) radiatively generates mass for the light neutrinos.
- Sizable parameter space over which electroweak vacuum remains stable upto M_{Pl}. perturbativity and unitarity constraints put stringent limits on the DM-SM Higgs coupling and the Z_2-odd scalar masses.

Conclusions

- In the first part, high-scale stability of the Type-II 2HDM scenario was examined.
- The *exact* $\mathbb{Z}_2$ symmetric model non-perturbative beyond 10 TeV. However, a broken $\mathbb{Z}_2$ needed to salvage high-scale validity all the way up to the M_{Pl}.
- In the second part, we have examined the high-scale validity of a scenario that (a) offers a scalar dark matter, (b) radiatively generates mass for the light neutrinos.
- Sizable parameter space over which electroweak vacuum remains stable upto M_{Pl}. perturbativity and unitarity constraints put stringent limits on the DM-SM Higgs coupling and the Z_2-odd scalar masses.
- Moreover, the role played by the heavy neutrinos in the RG evolution demonstrated. They induce corrections to the purely IDM beta functions, an effect which in turn reflected in the parameter spaces so obtained.

Conclusions

- In the first part, high-scale stability of the Type-II 2HDM scenario was examined.
- The *exact* $\mathbb{Z}_2$ symmetric model non-perturbative beyond 10 TeV. However, a broken $\mathbb{Z}_2$ needed to salvage high-scale validity all the way up to the M_{Pl}.
- In the second part, we have examined the high-scale validity of a scenario that (a) offers a scalar dark matter, (b) radiatively generates mass for the light neutrinos.
- Sizable parameter space over which electroweak vacuum remains stable upto M_{Pl}. perturbativity and unitarity constraints put stringent limits on the DM-SM Higgs coupling and the Z_2-odd scalar masses.
- Moreover, the role played by the heavy neutrinos in the RG evolution demonstrated. They induce corrections to the purely IDM beta functions, an effect which in turn reflected in the parameter spaces so obtained.

Thank you
for your attention

Model features: Scalar sector

- m_{11} and m_{22} eliminated using the tadpole conditions.
- The masses of the physical scalars,

$$
\begin{aligned}
m_A^2 &= \frac{m_{12}^2}{s_\beta c_\beta} - \frac{1}{2} v^2 \left(2\lambda_5 + \frac{\lambda_6}{t_\beta} + \lambda_7 t_\beta \right), \\
m_{H^\pm}^2 &= m_A^2 + \frac{1}{2} v^2 \left(\lambda_5 - \lambda_4 \right), \\
m_h^2 &= \frac{1}{2} \left[(A+B) - \sqrt{(A-B)^2 + 4C^2} \right], \\
m_H^2 &= \frac{1}{2} \left[(A+B) + \sqrt{(A-B)^2 + 4C^2} \right], \\
\tan 2\alpha &= \frac{2C}{A-B},
\end{aligned}
$$

where we have defined,

$$
\begin{aligned}
A &= m_A^2 s_\beta^2 + v^2(\lambda_1 c_\beta^2 + \lambda_5 s_\beta^2 + 2\lambda_6 s_\beta c_\beta), \\
B &= m_A^2 c_\beta^2 + v^2(\lambda_2 s_\beta^2 + \lambda_5 c_\beta^2 + 2\lambda_7 s_\beta c_\beta), \\
C &= -m_A^2 s_\beta c_\beta + v^2 \left[(\lambda_3 + \lambda_4) s_\beta c_\beta + \lambda_6 c_\beta^2 + \lambda_7 s_\beta^2\right].
\end{aligned}
$$

Constraints:Theoretical

- Vacuum stability: Stability of the electroweak vacuum is ensured up to some specified energy scale if the following conditions are satisfied for all scales Q up to that scale,

$$
\begin{aligned}
\mathrm{vsc1} &: \quad \lambda_1(Q) > 0 \\
\mathrm{vsc2} &: \quad \lambda_2(Q) > 0 \\
\mathrm{vsc3} &: \quad \lambda_3(Q) + \sqrt{\lambda_1(Q)\lambda_2(Q)} > 0 \\
\mathrm{vsc4} &: \quad \lambda_3(Q) + \lambda_4(Q) - |\lambda_5(Q)| + \sqrt{\lambda_1(Q)\lambda_2(Q)} > 0
\end{aligned}
$$

- Perturbativity:

$$\lambda_i(Q) < 4\pi$$

The corresponding constraints for the Yukawa and gauge interactions are,

$$y_i(Q),\ g_i(Q) < \sqrt{4\pi}$$

Results: $M_H > 500$ GeV regime

BP	M_H	$M_{H\pm}$	M_A	λ_L	λ_2
BP1	850.0 GeV	854.0 GeV	858.0 GeV	0.02	0.1
BP2	710.0 GeV	712.0 GeV	711.0 GeV	0.11	0.1

Table: Benchmark values (BP) of parameters affecting the RG evolution of the quartic couplings. For each BP, two values of M, namely, 110 TeV and 10^9 TeV, have been used.

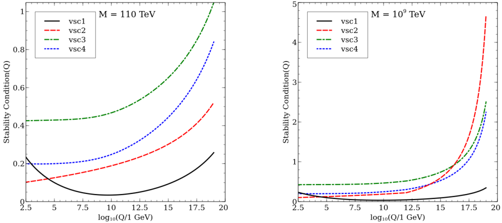

Figure: RG running of different scalar quartic couplings corresponding to BP1. The solid, dashed, dashed dotted and dotted lines denote the evolution curves of the stability conditions vsc1, vsc2, vsc3 and vsc4 respectively.

Results: $M_H > 500\ \mathrm{GeV}$ regime

- The theoretically allowed parameter space is fully consistent with the Higgs to diphoton LHC data in this case.
- The parameter space valid until the Planck scale and corresponding to $M = 110\ \mathrm{TeV}$ shrinks significantly for $M = 10^9\ \mathrm{TeV}$.
- Interestingly, y_ν becomes large $\mathcal{O}(10^{-1})$ for $M = 10^9\ \mathrm{TeV}$. Such a large yukawa coupling contributes to the beta function of λ_2 through the terms $+\lambda_2 y_\nu^2$ and $-y_\nu^4$ that either makes λ_2 perturbative in some cases or λ_2 negative and the vacuum unstable in other.
- The above argument best demonstrated through a display of RG evolution of λ_2.

Results: $M_H > 500$ GeV regime

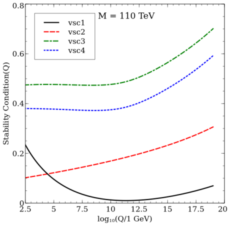

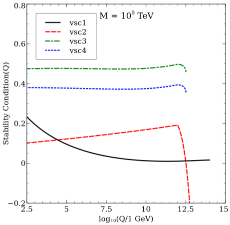

Figure: RG running of different scalar quartic couplings corresponding to BP2. The solid, dashed, dashed dotted and dotted lines denote the evolution curves of the stability conditions vsc1, vsc2, vsc3 and vsc4 respectively.

Constraints:Theoretical

- Unitarity: A further set of conditions come on demanding unitarity of the scattering matrix comprising all $2 \to 2$ channels involving, by the optical theorem. Each distinct eigenvalue (shown below) of the aforementioned amplitude matrix be bounded above at 8π.

$$
\begin{aligned}
a_\pm &= \frac{3}{2}(\lambda_1+\lambda_2) \pm \sqrt{\frac{9}{2}(\lambda_1-\lambda_2)^2+(2\lambda_3+\lambda_4)^2} \\
b_\pm &= \frac{1}{2}(\lambda_1+\lambda_2) \pm \sqrt{\frac{1}{4}(\lambda_1-\lambda_2)^2+\lambda_5^2}, \\
c_\pm &= d_\pm = \frac{1}{2}(\lambda_1+\lambda_2) \pm \sqrt{\frac{1}{4}(\lambda_1-\lambda_2)^2+\lambda_5^2}, \\
e_1 &= (\lambda_3+2\lambda_4-3\lambda_5), \\
e_2 &= (\lambda_3-\lambda_5), \\
f_1 &= f_2 = (\lambda_3+\lambda_4), \\
f_+ &= (\lambda_3+2\lambda_4+3\lambda_5), \\
f_- &= (\lambda_3+\lambda_5).
\end{aligned}
\tag{7}
$$

One-loop beta functions

The RG equations for the gauge couplings, for this model, are given by [**?**],

$$
\begin{aligned}
16\pi^2 \frac{dg_s}{dt} &= -7 g_s^3 , \\
16\pi^2 \frac{dg}{dt} &= -3 g^3 , \\
16\pi^2 \frac{dg'}{dt} &= 7 {g'}^3 .
\end{aligned}
$$

Here g', g and g_s denote the U(1), SU(2)$_L$ and SU(3)$_c$ gauge couplings respectively.

One-loop beta functions

$$
\begin{aligned}
16\pi^2 \frac{d\lambda_1}{dt} &= 12\lambda_1^2 + 4\lambda_3^2 + 4\lambda_3\lambda_4 + 2\lambda_4^2 + 2\lambda_5^2 + \frac{3}{4}(3g^4 + g'^4 + 2g^2g'^2) \\
&\quad -\lambda_1(9g^2 + 3g'^2 - 12y_t^2 - 12y_b^2 - 4y_\tau^2) - 12y_t^4 \,, \\
16\pi^2 \frac{d\lambda_2}{dt} &= 12\lambda_2^2 + 4\lambda_3^2 + 4\lambda_3\lambda_4 + 2\lambda_4^2 + 2\lambda_5^2 \\
&\quad + \frac{3}{4}(3g^4 + g'^4 + 2g^2g'^2) - 3\lambda_2(3g^2 + g'^2 - \frac{4}{3}y_\nu^2) - 4y_\nu^4 \,, \\
16\pi^2 \frac{d\lambda_3}{dt} &= (\lambda_1 + \lambda_2)(6\lambda_3 + 2\lambda_4) + 4\lambda_3^2 + 2\lambda_4^2 + 2\lambda_5^2 + \frac{3}{4}(3g^4 + g'^4 - 2g^2g'^2) \\
&\quad -\lambda_3(9g^2 + 3g'^2 - 6y_t^2 - 6y_b^2 - 2y_\tau^2 - 2y_\nu^2) \,, \\
16\pi^2 \frac{d\lambda_4}{dt} &= 2(\lambda_1 + \lambda_2)\lambda_4 + 8\lambda_3\lambda_4 + 4\lambda_4^2 + 8\lambda_5^2 + 3g^2g'^2 \\
&\quad -\lambda_4(9g^2 + 3g'^2 - 6y_t^2 - 6y_b^2 - 2y_\tau^2 - 2y_\nu^2) \,, \\
16\pi^2 \frac{d\lambda_5}{dt} &= (2\lambda_1 + 2\lambda_2 + 8\lambda_3 + 12\lambda_4)\lambda_5 - \lambda_5(9g^2 + 3g'^2 - 6y_b^2 - 2y_\tau^2 - 6y_t^2 -
\end{aligned}
$$

$$
\begin{aligned}
16\pi^2 \frac{dy_b}{dt} &= y_b \left(-8g_s^2 - \frac{9}{4}g^2 - \frac{5}{12}g'^2 + \frac{9}{2}y_b^2 + y_\tau^2 + \frac{3}{2}y_t^2 \right) , \\
16\pi^2 \frac{dy_t}{dt} &= y_t \left(-8g_s^2 - \frac{9}{4}g^2 - \frac{17}{12}g'^2 + \frac{9}{2}y_t^2 + y_\tau^2 + \frac{3}{2}y_b^2 \right) , \\
16\pi^2 \frac{dy_\tau}{dt} &= y_\tau \left(-\frac{9}{4}g^2 - \frac{15}{4}g'^2 + 3y_b^2 + 3y_t^2 + \frac{1}{2}y_\nu^2 + \frac{5}{2}y_\tau^2 \right) . \\
16\pi^2 \frac{dy_\nu}{dt} &= y_\tau \left(-\frac{9}{4}g^2 - \frac{3}{4}g'^2 - \frac{3}{4}y_\tau^2 + \frac{5}{2}y_\nu^2 \right) .
\end{aligned}
$$